

Progress in Understanding the Enigmatic Fast Radio Bursts

Shami Chatterjee^{1*}

¹*Cornell Center for Astrophysics and Planetary Science, Cornell University, Ithaca, NY 14853, USA*

Invited review for *Astronomy & Geophysics*

ABSTRACT

In less than a decade, fast radio bursts have gone from a single debated curiosity to a diverse extragalactic population with established host galaxies and energy scales. While a wide range of models remain viable, the central engines of FRBs are likely to involve energetic young magnetars, as confirmed by the recent discovery of a Galactic analog to these extragalactic bursts. Here we provide a brief introductory review of fast radio bursts, focusing on the rapid recent progress in observations of these enigmatic events, our understanding of their central engines, and their use as probes of the intergalactic medium. We caution against a rush to judgement on the mechanisms and classification of all FRBs: at this point, it remains plausible that there could be one dominant central engine, as well as the possibility that radio bursts are a generic feature produced by many different mechanisms. We also emphasize the importance of improved modeling of our Galaxy and Galactic halo, which otherwise impose systematic errors on every FRB line of sight. The future of science with fast radio bursts appears bright.

Key words: Fast Radio Bursts – Transients – Magnetars – Neutron Stars – Extragalactic Sources – Radio Astronomy

1 INTRODUCTION AND OVERVIEW

The time-domain radio sky is no longer *terra incognita*. Spurred on by advances in radio telescope sensitivity, bandwidth, resolution, and survey cadence, as well as huge leaps forward in computational capability and data storage, we now know of time variable phenomena on timescales spanning from years down to nanoseconds (Hankins et al. 2003), and operating on physical scales from parsecs to meters.

While periodic short-duration radio pulses have been known since the discovery of radio pulsars (Hewish et al. 1968), searches for isolated single pulses remained inconclusive (e.g., Linscott & Erkes 1980; Amy et al. 1989) until the discovery of rotating radio transients (RRATs, McLaughlin et al. 2006), which are now understood as Galactic pulsars with only occasionally-detectable pulses. These pulses all show a consistent dispersion, arriving earlier at high frequencies and later at lower frequencies due to their propagation through the cold tenuous plasma of interstellar space (see §2 and Figure 1 below), with an amount of dispersion consistent with an origin within our Milky Way galaxy.

Fast radio bursts are dispersed, isolated, millisecond-duration radio pulses similar in appearance to single pulses from Galactic pulsars, with the defining characteristic of a pulse dispersion measure that exceeds the maximum expected from our Galaxy in the originating direction. The first discovered fast radio burst (FRB) was identified in archival Parkes Multibeam survey data by Lorimer et al. (2007, see Figure 2 below), but the extragalactic origin suggested by its exceptional degree of pulse dispersion implied an enormous intrinsic brightness, making its astrophysical nature controversial, at least until further examples of FRBs were identified by Thornton et al. (2013).

Given the limited instantaneous field of view and on-sky time of typical high-time-resolution radio surveys, the detection of even a small number of short duration transient events is unlikely, and suggests that the true all-sky rate is enormous. Thornton et al. (2013) estimated a (detection threshold-dependent) event rate $\sim 1_{-0.5}^{+0.6} \times 10^4 \text{ sky}^{-1} \text{ day}^{-1}$, leading to a veritable gold rush of theoretical modeling efforts for central engines that accommodated both the enormous event rates and the high energy requirements for these millisecond flashes to be visible at cosmological (or at least extragalactic) distances.

The discovery of a repeating FRB at the Arecibo Observatory (FRB 20121102A; Spitler et al. 2014, 2016) immediately argued against a cataclysmic central engine, at least for some subset of FRBs, while its localization at the Karl G. Jansky Very Large Array (Chatterjee et al. 2017) and the measurement of the redshift of its dwarf host galaxy, $z \sim 0.2$, (Tendulkar et al. 2017) confirmed the extragalactic nature of these bursts and allowed a firm estimate of the isotropic equivalent energy budget for FRBs of $\sim 10^{38}$ erg. Since then, observations have progressed rapidly, with a large number of extremely bright bursts identified at the Australian SKA Pathfinder (ASKAP) telescope (Shannon et al. 2018), further localizations and host galaxy determinations (e.g., Bannister et al. 2019; Ravi et al. 2019b), and the Canadian Hydrogen Intensity Mapping Experiment (CHIME) detecting a bonanza of events (e.g., CHIME/FRB Collaboration 2019a), including further repeating sources (CHIME/FRB Collaboration 2019b,c). Meanwhile, although early theoretical models spanned the gamut from local flare stars (Loeb et al.

* E-mail: shami@astro.cornell.edu

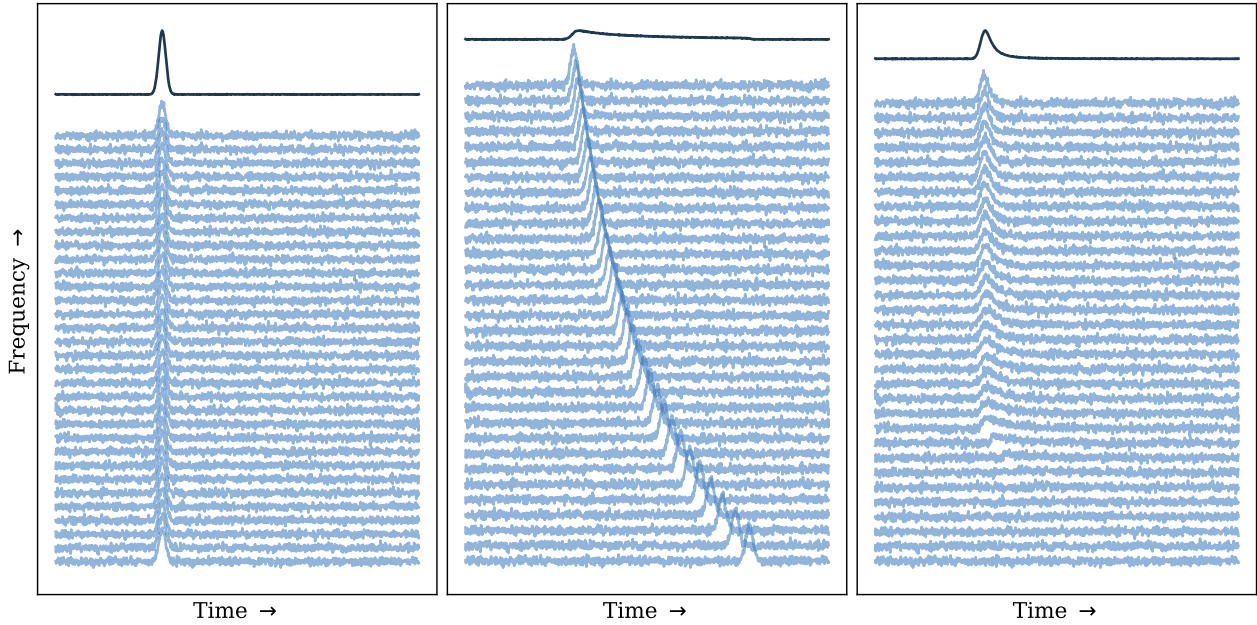


Figure 1. A burst or pulse (left panel) is dispersed (middle panel) and scattered (right panel) by propagation through an ionized medium. While both effects are frequency-dependent, dispersion is deterministic and can be reversed, while scattering can be understood as a convolution of the pulse with an interstellar medium transfer function, which does not necessarily allow for a unique deconvolution.

2014; Maoz et al. 2015) to cosmic strings (Vachaspati 2008), the most well-developed models feature very young neutron stars with extreme magnetic fields (magnetars, $B > 10^{14}$ G) embedded in their birth supernova remnants and/or their wind nebulae, with FRB emission arising from relativistic shocks in these nebulae (e.g., Lyubarsky 2014; Margalit & Metzger 2018; Margalit et al. 2020a; Beloborodov 2020).

Here we provide a brief and selective introduction to fast radio bursts, building on comprehensive recent reviews by Cordes & Chatterjee (2019) and Petroff et al. (2019). Zhang (2020) provides a recent compact overview of theoretical models, while an extensive collection of models is curated by Platts et al. (2019). For a blow-by-blow view from the front lines, we refer interested readers to the FRB Community Newsletter¹. Below we summarize propagation effects relevant to understanding FRBs (§2) and provide an overview of the FRB population (§3), repeating FRBs (§4), and host galaxy identifications and the use of FRBs as cosmological probes (§5). Finally, we describe a Galactic FRB event and its implications for the FRB central engine (§6), and conclude with an overview of future prospects for the field (§7).

2 PROPAGATION EFFECTS

Pulse dispersion: The interstellar medium (ISM) and intergalactic medium (IGM) both consist of cold, tenuous, magnetized plasma, which imposes a frequency-dependent delay on the time of arrival of a pulse, $\Delta t \propto DM \nu^{-2}$, where the dispersion measure DM is the integrated column density of electrons n_e along the line of sight:

$$DM = \int_0^L n_e ds,$$

weighted by $(1+z)^{-1}$ for the cosmological case. As illustrated in Figure 1, dispersion results in a smeared-out pulse in the time domain, making detection unlikely unless the DM is fit for and removed first. If the baseband radio signal can be sampled with high enough time resolution, the effect of a known (or trial) DM can be deterministically removed. Otherwise, the channelized time-frequency data can be searched over in increments of DM, at the cost of some residual intra-channel smearing that reduces the significance of a detected pulse. The latter is more typical for present-day blind searches, due to the computational cost of working with baseband data.

Pulses from Galactic radio pulsars show consistent values of DM over long periods of time (with small variations due to interstellar “weather”) and with enough pulsars at known distances, the known values of the integrated electron column density can be used to map out the Galactic electron density distribution (Taylor & Cordes 1993). Electron density distribution models such as NE2001 (Cordes & Lazio 2002) and YMW16 (Yao et al. 2017) are widely used to determine whether the DM of a pulse or burst can be accounted for within the Milky Way, or if it is more likely to be of extragalactic origin. After accounting for the contributions of the Milky Way disk and halo, as well as the ISM of the host galaxy, extragalactic burst DMs quantify the integrated column density of the IGM, allowing for a census of the baryons in that tenuous gas (e.g., Macquart et al. 2020).

¹ FRB Community Newsletter: <http://frb.astro.cornell.edu/news/>

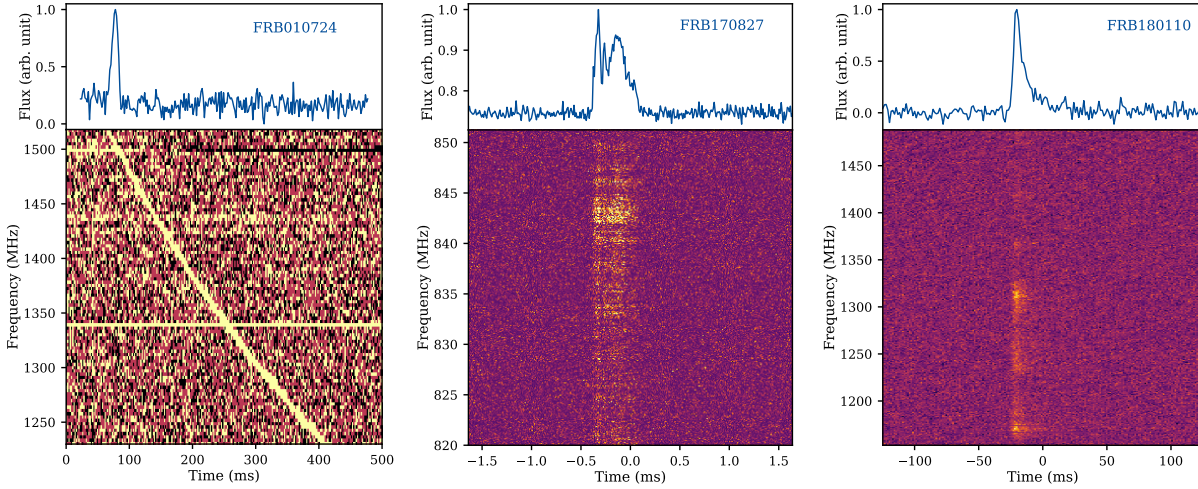


Figure 2. Examples of fast radio burst dynamic spectra. Left: FRB 010724, the first reported example (Lorimer et al. 2007), with $DM = 375 \text{ pc cm}^{-3}$. The lower panel shows the burst dispersion sweep in the time-frequency plane; after removing the best fit dispersion sweep, the frequency-averaged burst profile is shown in the upper panel. Middle: FRB 170827, detected at UTMOST (Farah et al. 2018). The lower panel shows the dynamic spectrum after removal of the dispersion sweep, $DM = 177 \text{ pc cm}^{-3}$. Voltage capture was triggered after real-time detection, revealing time-frequency scintillation structure in the burst after coherent de-dispersion. The upper panel shows the frequency-averaged burst profile. Right: FRB 180110, a bright burst detected at ASKAP (Shannon et al. 2018) and shown after removal of the dispersion sweep with $DM = 716 \text{ pc cm}^{-3}$. Note the scattering tail and the scintillation structure.

Scattering and Scintillation: Electron density fluctuations on scales larger than a wavelength can lead to small-angle scattering, leading to strongly frequency-dependent pulse scattering ($\propto \nu^{-4}$), as shown in Figure 1. That can be understood as multi-path propagation leading to a smearing of the pulse (as well as angular broadening of the source image), or as a convolution of the pulse or burst with a (frequency-dependent) propagation transfer function in the time domain. Like other convolution processes, scattering does not necessarily allow for unique deconvolution.

Along with scattering, pulses can show both refractive and diffractive scintillation due to propagation through a turbulent medium. Diffractive interstellar scintillation, the radio analog of stellar twinkling due to turbulence in the Earth’s atmosphere, can produce up to 100% modulation in the spectrum of a burst, producing band-limited structures in the dynamic spectrum. Scintillation and scattering effects are often apparent in the spectra of FRBs, as shown in Figure 2, and have been used to probe the turbulence spectrum of the ionized IGM (e.g., Ravi et al. 2016).

Plasma Lensing: Density structure in the host galaxies of FRBs can act as plasma lenses, producing frequency-dependent focusing and defocusing at the detector, as described by Cordes et al. (2017). Such lensing would be the extragalactic equivalent of the Galactic “extreme scattering events” (Fiedler et al. 1987). Large magnification factors up to $\sim 10^2$ are possible over short timescales (hours to days) and narrow frequency ranges (0.1–1 GHz), if the detector location falls on a caustic.

Faraday Rotation: The left- and right-hand circularly polarized components of a radio wave have different refractive indices in the magnetized plasma of the ISM and IGM, and travel at different speeds, leading to a wavelength-dependent rotation of the observed linear polarization angle θ compared to the angle at emission, $\Delta\theta = RM\lambda^2$, for wavelength λ . RM, the rotation measure, is given by the integral of the component of the magnetic field along the line of sight, weighted by the electron density:

$$RM \propto \int_0^L B_{\parallel} n_e ds.$$

Thus a burst or pulse with detectable linear polarization can be used to trace the integrated density-weighted magnetic field along the line of sight, including the magnetic field in the IGM and the host galaxy environment (Masui et al. 2015; Ravi et al. 2016; Michilli et al. 2018).

3 THE POPULATION OF FAST RADIO BURSTS

Standard searches for single pulses and bursts operate on dynamic spectra acquired at radio telescopes with high time and frequency resolution. The data are typically cleaned of interference, calibrated for the instrumental bandpass response, de-dispersed at trial values of DM, and frequency averaged, with the resulting time series being inspected for departures from random noise. Advances in computational capability and storage capacity have allowed for the exploration of many variations on this basic approach, including the development of the fast discrete dispersion measure transform (FDMT; Zackay & Ofek 2017) and the use of Graphical Processing Units, machine learning, and computer vision approaches (e.g., FETCH; Agarwal et al. 2020). Real-time searches have allowed for the capture of buffered voltage data, allowing for coherent dedispersion of newly-detected FRBs (e.g., Price et al. 2019; Farah et al. 2018 and Figure 2).

Radio frequency interference (RFI) is the bane of all of these searches. With interference sources ranging from the local (unshielded elec-

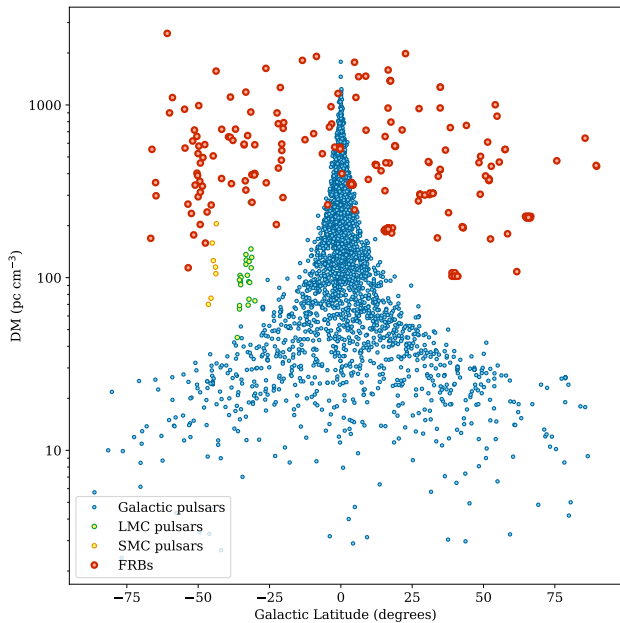


Figure 3. Pulse dispersion measure distinguishes FRBs from pulsars. In this updated version of a plot presented by Cordes & Chatterjee (2019), DM is plotted against Galactic latitude for Galactic pulsars (2751 objects) and pulsars in the LMC (22 objects) and SMC (7 objects), as obtained from the Pulsar Catalogue (Manchester et al. 2005), as well as for FRBs (284 bursts, from the Transient Name Server service). The DM envelope of the Milky Way is clearly apparent.

tronics and computers, automobile spark plugs) to the global (constellations of low-earth orbit satellites), the radio spectrum is an increasingly endangered resource overwhelmed by commercial pressure. Beyond relying on the dispersive sweep of astrophysical signals, RFI excision algorithms have become more sophisticated over time, but transient signals are frequently swamped by false positive candidates from interference.

Examples of FRB dynamic spectra and dispersion-corrected intensity profiles are shown in Figure 2. As of December 2020, there are 284 FRB events (including repeat bursts) recorded by the Transient Name Server (TNS²), the official IAU repository. Collectively, their DMs show a clear separation from the Galactic pulsar population (Figure 3), emphasizing their extragalactic nature. Estimates for the rates of FRB events depend on the sensitivity threshold, with recent estimates ranging from 37 ± 8 events $\text{sky}^{-1} \text{day}^{-1}$ brighter than 29 Jy-ms (Shannon et al. 2018) to $1.7_{-0.9}^{+1.5} \times 10^3$ events $\text{sky}^{-1} \text{day}^{-1}$ brighter than 2 Jy-ms (Keane et al. 2018; Bhandari et al. 2018). However, these estimates are complicated by the fact that most surveys have varying RFI environments, and single-dish radio telescopes have large low-sensitivity sidelobes which could pick up very bright bursts. In any case, the current numbers and rate estimates will soon be rendered obsolete by upcoming results from CHIME, which surveys the sky on a daily transit basis, as discussed further below.

Likewise, understanding the fluence distribution of detected FRBs is complicated for all cases that lack a precise localization from interferometric detection, because of the beam response function (and sidelobes) of single dish telescopes. However, it is safe to say that the current statistics of FRBs are incomplete in every parameter — fluence, burst width, event rate, DM distribution, repetition, polarization, and more (e.g., Ravi 2019b). There is more to be learned.

4 REPEATING FAST RADIO BURSTS

The discovery that FRB 20121102A (hereafter FRB 121102) was a repeating source (Spitler et al. 2016; Scholz et al. 2016, and Figure 4) dramatically altered the FRB landscape. While immediately ruling out cataclysmic events as the central engine for at least some FRBs, it suggested the existence of at least two classes of FRBs, in analogy with long and short gamma ray bursts (GRBs, Kouveliotou et al. 1993), as well as the possibility that FRB 121102 was a singular outlier.

A repeating source also allows targeted follow-up observations, and coherent dedispersion at the known DM reveals spectral details at high resolution. As shown in Figure 4, FRB 121102 shows a diversity of burst morphologies, including single bright sharply-peaked bursts, faint smudges at the detection threshold (Gourdji et al. 2019), and downward-drifting islands of emission in the dynamic spectrum after removal of dispersion (Hessels et al. 2019), now commonly referred to as the “sad trombone” effect and possibly a signature of plasma lensing. FRB 121102 has been detected at frequencies as high as 4–8 GHz (Gajjar et al. 2018) and as low as 0.4–0.8 GHz (Josephy et al. 2019), with event rates as high as 45 bursts in 30 minutes (Zhang et al. 2018) but no detection of periodicity. Simultaneous multiwavelength observations

² TNS: <https://wis-tns.weizmann.ac.il/>

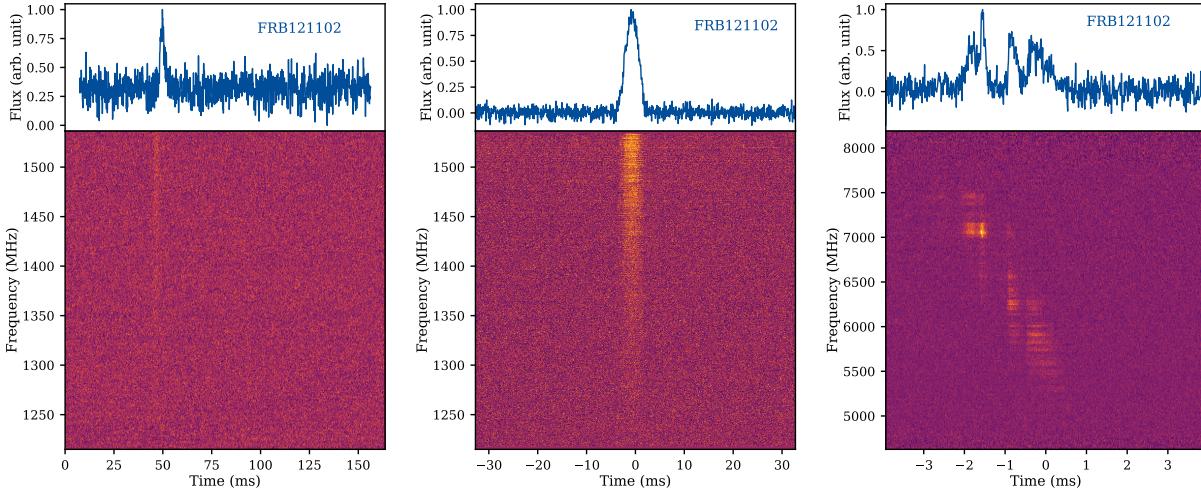


Figure 4. Three bursts from the repeating FRB 121102. As before, lower panels show the dynamic spectrum after removal of the best-fit dispersion sweep, and the upper panels show the frequency-averaged burst profile. Left: The faint original detection at Arecibo (Spitler et al. 2014), showing an inverted spectrum. Middle: One of the brightest repeat bursts from FRB 121102 detected at Arecibo (Spitler et al. 2016). Right: A detection at the Green Bank telescope at 4–8 GHz (Gajjar et al. 2018), showing extensive downward-drifting structure in the time-frequency plane (the “sad trombone”) after removal of the dispersion sweep.

have revealed no burst counterparts in X-rays, gamma-rays, or optical bands (Scholz et al. 2016; Hardy et al. 2017; Acciari et al. 2018), although given the millisecond durations of the bursts, the limits are not energetically constraining.

The bursts from FRB 121102 also appear almost completely linearly polarized, with a Faraday rotation measure that is high ($> 10^5$ rad m^{-2}) and varying over time (Michilli et al. 2018). The changing RM, without correspondingly significant changes in DM, implies that the projected component of the magnetic field is changing over time, and that the source is embedded in an extreme magneto-ionic medium. Indeed, the only comparable phenomenology, among all the known pulsars in our Galaxy, is seen for the Galactic center magnetar J1745–2900 (Desvignes et al. 2018), in the neighborhood of Sgr A*.

The discovery of multiple repeating FRB sources at CHIME (CHIME/FRB Collaboration 2019b,c; Fonseca et al. 2020) confirmed that a fraction of FRBs were detectable as repeating sources, indistinguishable in their DM distributions from the rest of the population, although their burst widths were somewhat larger on average and showed the “sad trombone” effect in several cases.

The CHIME repeating FRB 20180916B (hereafter FRB 180916) is of particular interest. While no repeating FRB source has yet been demonstrated to be periodic, FRB 180916 shows periodic windows of detectability (CHIME/FRB Collaboration 2020a), with a ~ 5.2 -day window every 16.3 days during which bursts may (or may not) be detected. Such behavior immediately suggests a binary orbit (e.g., Lyutikov et al. 2020; Ioka & Zhang 2020), or precession (e.g., Levin et al. 2020; Zanazzi & Lai 2020; Sob’yanin 2020), or possibly a very slow underlying rotation period (Beniamini et al. 2020) for the central engine. A similar but wider ($\sim 56\%$) periodic detectability window has also been claimed for FRB 121102, with a period of ~ 157 days (Rajwade et al. 2020; Cruces et al. 2020).

Recent detections of the repeating FRB 180301 with the Five-hundred-meter Aperture Spherical radio Telescope (FAST) have revealed a high degree of linear polarization, comparable to that seen for FRB 121102. However, these bursts show a wide variety of polarization angle swings (Luo et al. 2020), a puzzling observation that appears inconsistent with models for FRB production in relativistic shocks (Lyubarsky 2014; Margalit & Metzger 2018; Beloborodov 2020). Instead, Luo et al. (2020) argue that the bursts are produced in neutron star magnetospheres, as suggested by many other models (e.g. Katz 2014; Cordes & Wasserman 2016; Kumar et al. 2017; Zhang 2017).

Could all FRBs be repeating sources, or are they two separate classes? It has been apparent from the first FRB rate estimates that cataclysmic phenomena alone cannot account for the event rate (Ravi 2019a), but in spite of very deep follow-up observations (e.g., Petroff et al. 2015b; Shannon et al. 2018), demonstrating that a source never repeats is impossible, and current constraints are limited in nature (Caleb et al. 2019a; James et al. 2020; and see §2.2, “Follow-up Observations: Trials and Tribulations” in Cordes & Chatterjee 2019). FRB 121102, a prolific repeater at higher frequencies (Gajjar et al. 2018), has been detected only once so far at 400–800 MHz, in spite of daily transits at CHIME (Joseph et al. 2019). FRB 20190711A, an ASKAP-detected burst, has been seen to repeat in deep observations at Parkes, but in an extremely band-limited manner, occupying only 65 MHz of a 3.3 GHz bandwidth (Kumar et al. 2021). These observational selection effects argue against a definitive answer to the question at present, although repeating FRBs have not (yet) shown any circularly polarized radio emission, and Dai et al. (2020) propose that feature as a key discriminant between repeating and non-repeating classes, indicative of different radiation mechanisms. However, given the inventiveness of Nature, fast radio bursts might all still have the same underlying engine, or may turn out to be a generic feature from many different source classes.

5 LOCALIZATION AND HOST GALAXIES

The measurement of source distances is a fundamental problem in astronomy, and FRBs have been no exception. Understanding the energetics of FRB central engines, or using FRBs as cosmological probes, requires a distance measurement, most plausibly through the redshift of a host galaxy. However, until large scale surveys started with ASKAP and CHIME, most FRBs were detected by single dish radio telescopes with few-arcminute resolution, while a robust host galaxy association requires few-arcsecond localization (Eftekhari & Berger 2017; Eftekhari et al. 2018). Also, in spite of enormous efforts devoted to real-time detection of FRBs and multiwavelength follow-up (e.g., Petroff et al. 2015a, 2017), no reliable counterparts were identified at other bands.

The first direct localization of a fast radio burst (FRB 121102, Chatterjee et al. 2017) relied on VLA interferometric follow-up of the first source known to repeat. The identification of a star-forming dwarf galaxy host (Figure 5) and the measurement of its redshift, $z = 0.193$ (Tendulkar et al. 2017) allowed a firm estimate of the burst energetics from the fluence A_ν of detected bursts,

$$E_{\text{burst}} = 4\pi D^2 (\delta\Omega/4\pi) A_\nu \Delta\nu \approx 10^{38} \text{ erg } (\delta\Omega/4\pi) D_{\text{Gpc}}^2 (A_\nu/0.1 \text{ Jy ms}) \Delta\nu_{\text{GHz}},$$

where the distance $D \sim 1$ Gpc and the unknown beaming solid angle $\delta\Omega$ scales the total energy requirement. Note, however, that while a narrower beam reduces the energy budget per source, it requires a corresponding increase in the number of such sources. In any case, the energetics are compatible with neutron stars or other compact object progenitors. In addition, a persistent radio source is associated with the bursts at milliarcsecond scales (Chatterjee et al. 2017; Marcote et al. 2017). While the persistent radio source is not inconsistent with a (weak) active galactic nucleus (Vieyro et al. 2017), it is naturally explained as a nebula surrounding a very young magnetar in a concordance model for FRB 121102 (Margalit & Metzger 2018), consistent with its association with a star-forming region in the host galaxy (Bassa et al. 2017).

However, this self-consistent picture has not proven to be universal. Interferometric localizations of one-off FRBs with ASKAP (Bannister et al. 2019; Prochaska et al. 2019; Macquart et al. 2020; Bhandari et al. 2020; Heintz et al. 2020) as well as the DSA-10 (Ravi et al. 2019b) and the VLA (Law et al. 2020) led to the identification of a diversity of host galaxies in morphology and metallicity, as well as diverse environments within the galaxies themselves, as illustrated for a sample in Figure 5.

Even the second repeating FRB to be localized, the CHIME-detected FRB 180916, was localized with EVN observations to a nearby, massive spiral galaxy (Marcote et al. 2020, see Figure 5), with no associated persistent radio source detected in spite of its low redshift ($z = 0.034$) and distance (149 Mpc). With high-resolution optical observations, Tendulkar et al. (2020) show that the source, with its periodic detectability windows described above, is not associated with a star-forming region and inconsistent with even a runaway magnetar, and suggest that the source may instead be a high-mass X-ray (or gamma-ray) binary.

Alongside the quest to understand the central engine behind FRB emission, the promise of FRBs with well-measured distances is the ability to directly probe the baryon content of the IGM (e.g., Ioka 2003; Inoue 2004; McQuinn 2014; Prochaska & Zheng 2019). At low redshift, the vast majority of the baryon content of the universe is not seen (the so-called “missing baryon problem”; e.g., Bregman 2007) but is believed to lie in gaseous filaments between galaxy clusters. As shown in Figure 6, the extragalactic DM component of FRBs correlates with the host galaxy redshift.

Note, however, the scatter about a simple linear trend in Figure 6. The measured DM of each FRB includes contributions from the Milky Way, subject to modeling uncertainties in NE2001 (Cordes & Lazio 2002) or YMW16 (Yao et al. 2017). The contribution of the Milky Way halo is not well known, with a range of plausible values spanning $50 \pm 25 \text{ pc cm}^{-3}$ (e.g., Prochaska & Zheng 2019). The host galaxy (and its halo) will also contribute similar amounts to the total DM, and these contributions (weighted for redshift) have to be accounted for before a redshift-DM relationship can be measured. In a first such effort, Macquart et al. (2020) use a carefully-selected sample of FRBs to estimate the cosmic baryon density and show consistency with cosmological predictions. The uncertainties are large at present, but can be refined with enough well-measured FRBs. In addition, FRBs also probe galaxy or cluster halos along the line of sight (e.g., Connor et al. 2020) and a large enough sample of FRBs may allow detailed tomographic modeling of nearby clusters (Ravi et al. 2019a). In order to realize the promise of FRBs as extragalactic probes, it is crucial to improve modeling of the electron density distribution in the Galaxy (e.g. Ocker et al. 2020) and the Galactic halo.

6 A GALACTIC FRB AND THE FRB CENTRAL ENGINE

As discussed above, there are a diverse range of models for FRBs (see, e.g., Zhang 2020) but compact objects (and specifically young magnetars) are implicated in most viable ones. The association of a compact persistent radio source with FRB 121102, along with its high rotation measure, favors models where the FRB emission arises from relativistic shocks in the nebula surrounding the neutron star, but such a persistent source is not seen for the nearby repeating FRB 180916. In contrast, the periodic detectability of FRB 180916 (and possibly FRB 121102) can be naturally explained by an orbit, precession, or very slow rotation; and the varying polarization angle swings for the repeating FRB 180301 suggest a magnetospheric origin for the bursts. The situation appears (delightfully) unsettled, although the FRB sample with secure host galaxy associations is consistent with an origin in a population of magnetars (Bochenek et al. 2020a; Heintz et al. 2020). That naturally raises the prospect of detecting FRBs from magnetars in our own Galactic backyard, although with the caveat that such a burst might be so bright that it would be flagged and excised as radio interference.

Such a prospect has been spectacularly confirmed with the recent detection of radio bursts from the Galactic magnetar SGR 1935+2154. Magnetars are known to produce gamma-ray bursts and giant X-ray flares, quasi-periodic activity, periodic radio pulses, and more (Kaspi

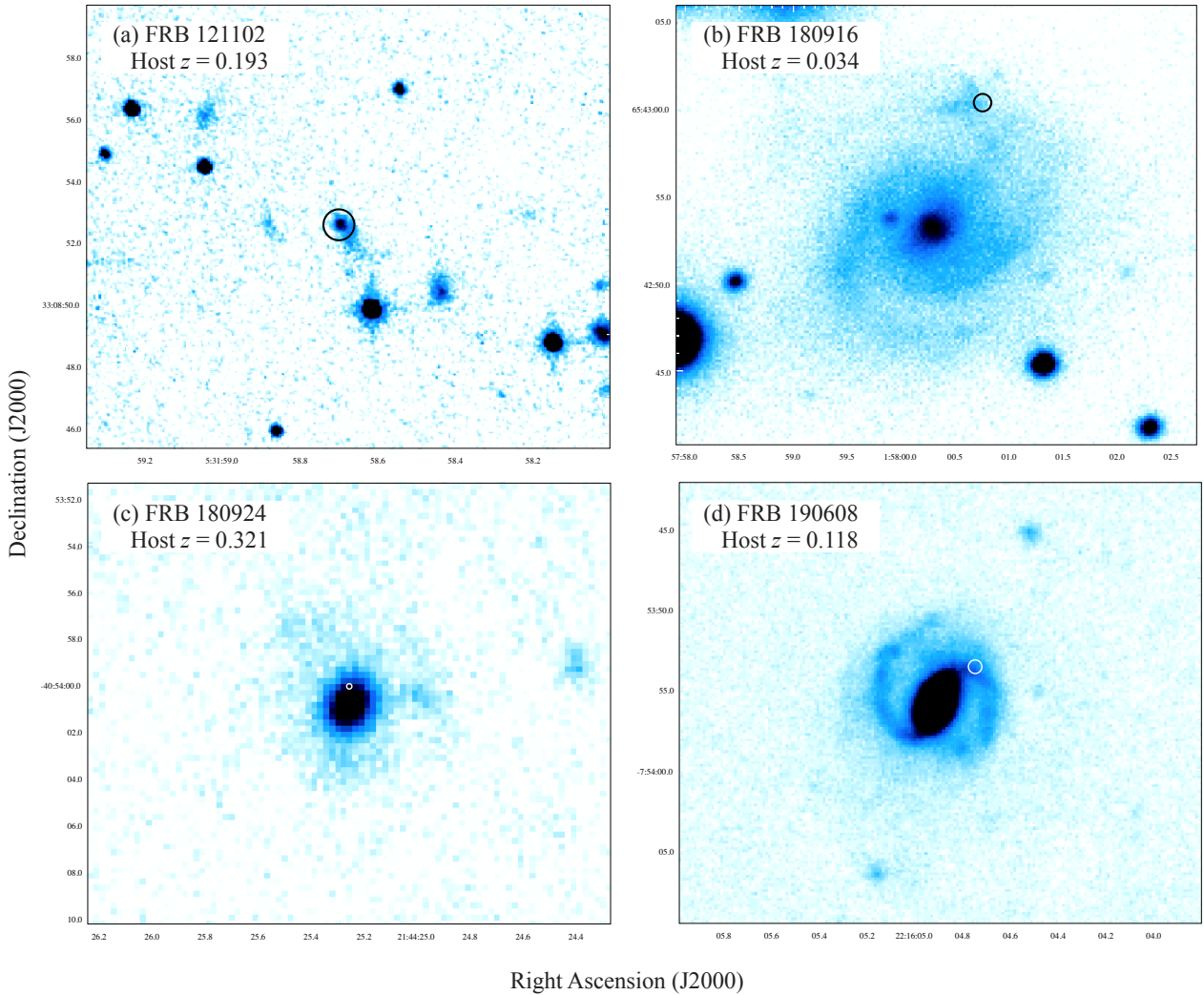


Figure 5. FRB host galaxies show a diversity of morphologies. (a) The dwarf host galaxy of the repeating FRB 121102, at $z = 0.193$ (Tendulkar et al. 2017), as imaged with the Hubble Space Telescope WFC3 in the F110W (J-band) filter (Bassa et al. 2017). The localization region is indicated with a circle of radius $0''.5$; the position is known to milliarcsecond precision (Chatterjee et al. 2017; Marcote et al. 2017). (b) The nearby spiral host galaxy of the repeating FRB 180916, at $z = 0.034$ (Marcote et al. 2020), as imaged with Gemini-North at r' -band. As in (a), the localization region is indicated with a circle of radius $0''.5$, although the position is known to milliarcsecond precision. (c) FRB 180924, a single burst detected at ASKAP, is localized to a luminous lenticular or early spiral galaxy at $z = 0.321$ (Bannister et al. 2019), as imaged with VLT/FORS2 at g -band. The localization uncertainty radius is $0''.11$. (d) FRB 190608 is another single ASKAP-detected burst, localized to a nearby spiral galaxy at $z = 0.118$ (Macquart et al. 2020) with a localization uncertainty radius of $0''.42$, as imaged with VLT/X-shooter at g -band.

& Beloborodov 2017), primarily driven by the potential energy stored in their extreme magnetic fields ($B > 10^{14}$ G). While the magnetar SGR 1935+2154 was in an extended “active” phase, producing hundreds of X-ray flares (see Weltman & Walters 2020 for a timeline of events), an extremely intense two-component radio burst was detected by CHIME at 400-800 MHz (CHIME/FRB Collaboration 2020b) with a combined fluence of 700 kJy ms and a DM of 332.7 pc cm^{-3} . Coincident with that burst, a burst was detected at the STARE2 array at 1.4 GHz (Bochenek et al. 2020b) with a fluence of 1.5 MJy ms and the same DM. The burst dynamic spectra are shown in Figure 7 after removal of the pulse dispersion; these bursts were bright enough to have been detected and unambiguously classified as FRBs if they had been beamed towards us from nearby galaxies.

Several satellites also detected a bright, hard X-ray burst coincident with the radio burst (after accounting for pulse dispersion delays) among a forest of other X-ray bursts (for example, AGILE; Tavani et al. 2020), suggesting that the radio emission had a much narrower beaming angle than the X-rays did. Observations at FAST also placed upper limits on any pulsed radio emission (Lin et al. 2020), although a few fainter bursts were detected (Kirsten et al. 2020), suggesting a possible continuum of bursts extending down to much weaker fluences (at least 7 orders of magnitude).

While the detection of radio bursts from SGR 1935+2154 confirms that magnetars produce at least some fraction of FRBs, there still exists a $30\times$ difference in intrinsic energy between the bright burst seen at STARE2 and even the weaker known FRBs, so the provenance of the

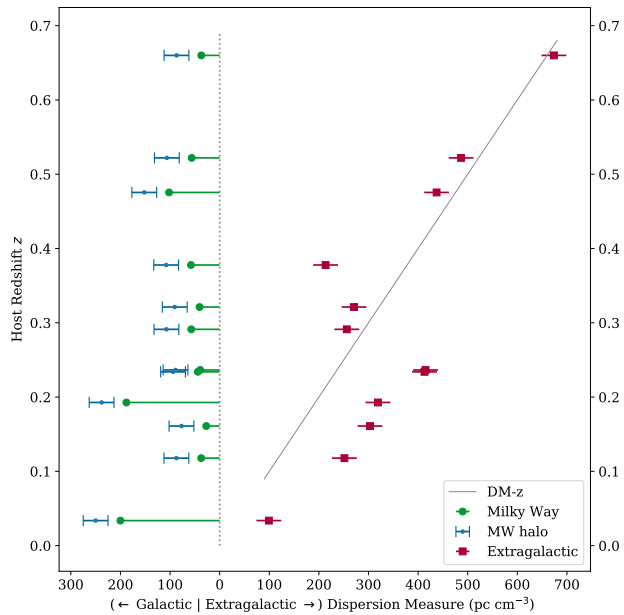


Figure 6. The Galactic and extragalactic components of FRB dispersion measure plotted against the FRB host galaxy redshift. The Milky Way contribution from NE2001 is shown on the left, along with a nominal Milky Way halo contribution of $50 \pm 25 \text{ pc cm}^{-3}$. The extragalactic DM includes an unknown host galaxy contribution, with the uncertainty due to the Milky Way halo contribution shown for emphasis. A line is plotted to indicate an approximate relationship $\text{DM} \approx 1000 z \text{ pc cm}^{-3}$ for the IGM at low z (e.g., [McQuinn 2014](#)), to which host galaxy contributions should add on.

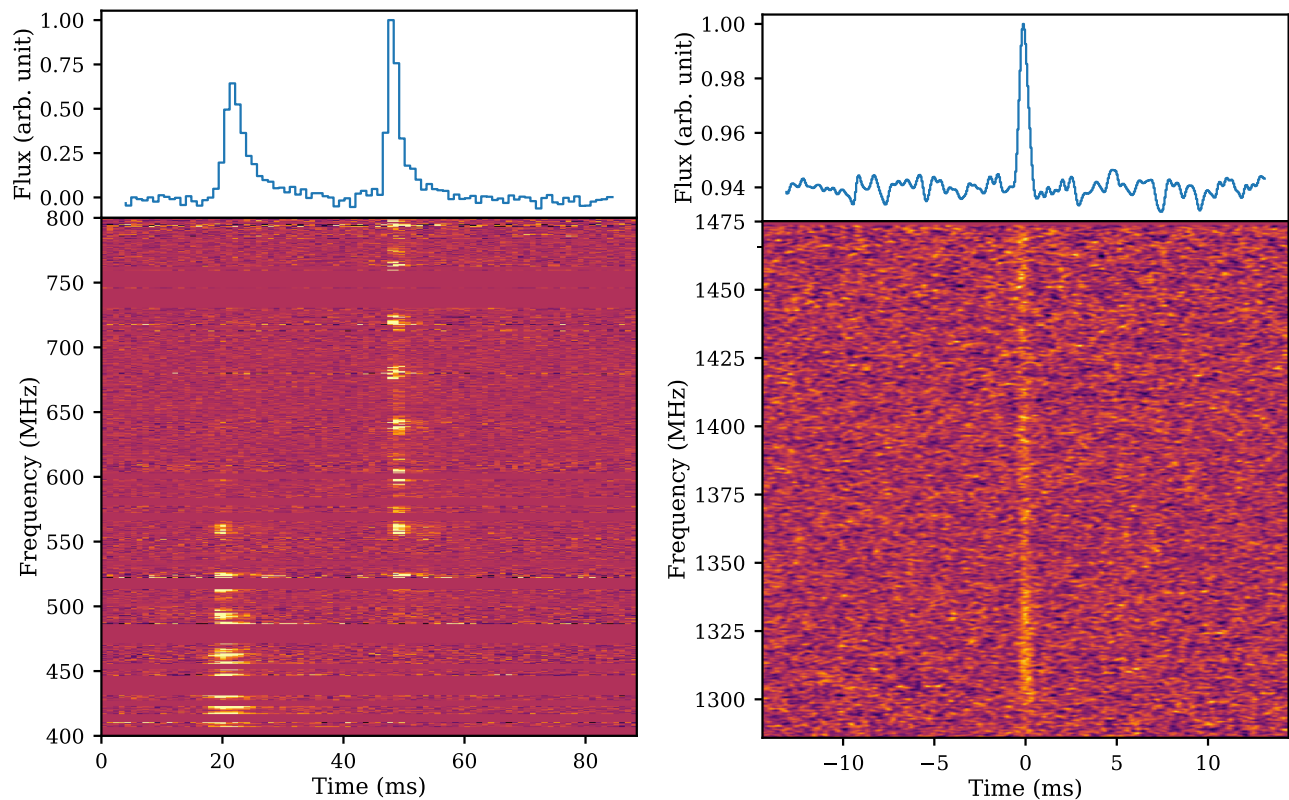


Figure 7. Radio burst from SGR 1935+2154, as detected at (left) CHIME at 400–800 MHz ([CHIME/FRB Collaboration 2020b](#)), and (right) STARE2 at 1.4 GHz ([Bochenek et al. 2020b](#)). Time axis labels have an arbitrary offset; the higher (second) peak of the CHIME burst is aligned with the STARE2 burst in time after correcting for dispersive delays at the different frequencies.

brightest FRBs remains a somewhat open question. [Margalit et al. \(2020b\)](#) argue that the properties of the coincident radio and X-ray flares from SGR 1935+2154 are consistent with the predictions of the synchrotron maser shock model rather than arising in the magnetosphere, but propose an additional population of extremely active magnetars with even stronger magnetic fields to account for the observed FRB rate and repeating fraction. A unified model for the weaker Galactic magnetar bursts and the brighter cosmological FRBs is proposed by [Lu et al. \(2020\)](#), who invoke magnetic disturbances propagating outwards from near the magnetar surface to produce radio bursts.

We note, for now, that the number of models exceeds the number of observational constraints and that no single model yet explains all the observed phenomenology of FRBs, including the volumetric rates, morphology differences, repeatability, periodic detectability windows, polarization properties, and more. The prospect remains open that FRB emission could arise from multiple engines, or from several closely related source classes, although the likelihood is high that magnetars (or other neutron stars) are central to the process.

7 FUTURE PROSPECTS

In less than a decade, fast radio bursts have gone from a single debated curiosity to a diverse extragalactic population with established host galaxies and energy scales. While a wide range of models remain viable, the central engines of FRBs are likely to involve energetic young magnetars, as confirmed by the recent discovery of a Galactic analog to these extragalactic bursts. However, we caution against a rush to judgement on the mechanisms and classification of all FRBs: at this point, it remains plausible that there could be one dominant central engine, as well as the possibility that radio bursts are a generic feature produced by many different mechanisms.

FRBs are already being used to probe the halos of other galaxies ([Prochaska & Zheng 2019](#); [Connor et al. 2020](#)) and to address the distribution of baryons in the IGM ([Macquart et al. 2020](#)). In future, the availability of a large sample of well-characterized FRBs with host galaxies may be used to address a broad range of topics (e.g., [Ravi et al. 2019a](#)), including measurement of the IGM magnetic field ([Akhori et al. 2016](#)), the cosmological baryon density at intermediate redshifts ([Walters et al. 2018](#)), and the era of helium reionization ([Caleb et al. 2019b](#)). FRB microlensing can reveal the presence of massive compact halo objects as a constituent of dark matter ([Muñoz et al. 2016](#)).

In order to live up to this promise, many more FRBs need to be detected. In this regard, the ongoing transit sky survey with CHIME is likely to be transformative, with hundreds of detected FRBs and a well-defined sky exposure map that will allow for robust statistical analyses. Further, while FRB detections are interesting in their own right, the bursts need to be localized to \sim arcsecond precision and host galaxy redshifts measured in order to unlock their potential as probes of the IGM density and magnetic field. Interferometric surveys with ASKAP, the DSA-10, and the VLA have already demonstrated localizations from one-off detections, with similar efforts underway at other interferometers (UTMOST-2D, DSA-110, MeerKAT, and more). In future, very long baseline interferometry at the EVN, VLBA, and eventually the CHIME outriggers have the potential to associate one-off FRB detections not just with host galaxies, but with specific regions that allow constraints on their progenitors, as already demonstrated for repeating FRBs. Closer to home, we also emphasize the importance of improving the modeling of our Galaxy and Galactic halo, which otherwise impose systematic errors on every FRB line of sight. The future of science with fast radio bursts appears bright.

ACKNOWLEDGEMENTS

The author thanks Jim Cordes, Emily Petroff, and many other colleagues, especially in the CHIME and NANOGraV collaborations, for extensive discussions and access to data. The author acknowledges support from the National Science Foundation (AAG 1815242), and is a member of the NANOGraV Physics Frontiers Center, which is supported by the National Science Foundation award number 1430284.

REFERENCES

- Acciari V. A., et al., 2018, *MNRAS*, p. 2306
 Agarwal D., Aggarwal K., Burke-Spolaor S., Lorimer D. R., Garver-Daniels N., 2020, *MNRAS*, 497, 1661
 Akahori T., Ryu D., Gaensler B. M., 2016, *ApJ*, 824, 105
 Amy S. W., Large M. I., Vaughan A. E., 1989, *Proceedings of the Astronomical Society of Australia*, 8, 172
 Bannister K. W., et al., 2019, *Science*, 365, 565
 Bassa C. G., et al., 2017, *ApJ*, 843, L8
 Beloborodov A. M., 2020, *ApJ*, 896, 142
 Beniamini P., Wadiasingh Z., Metzger B. D., 2020, *MNRAS*, 496, 3390
 Bhandari S., et al., 2018, *MNRAS*, 475, 1427
 Bhandari S., et al., 2020, *ApJ*, 895, L37
 Bochenek C. D., Ravi V., Dong D., 2020a, arXiv e-prints, p. arXiv:2009.13030
 Bochenek C. D., Ravi V., Belov K. V., Hallinan G., Kocz J., Kulkarni S. R., McKenna D. L., 2020b, *Nature*, 587, 59
 Bregman J. N., 2007, *ARA&A*, 45, 221
 CHIME/FRB Collaboration 2019a, *Nature*, 566, 230
 CHIME/FRB Collaboration 2019b, *Nature*, 566, 235
 CHIME/FRB Collaboration 2019c, *ApJ*, 885, L24
 CHIME/FRB Collaboration 2020a, *Nature*, 582, 351

- CHIME/FRB Collaboration 2020b, *Nature*, **587**, 54
- Caleb M., Stappers B. W., Rajwade K., Flynn C., 2019a, *MNRAS*, **484**, 5500
- Caleb M., Flynn C., Stappers B. W., 2019b, *MNRAS*, **485**, 2281
- Chatterjee S., et al., 2017, *Nature*, **541**, 58
- Connor L., et al., 2020, *MNRAS*, **499**, 4716
- Cordes J. M., Chatterjee S., 2019, *ARA&A*, **57**, 417
- Cordes J. M., Lazio T. J. W., 2002, arXiv e-prints, pp astro-ph/0207156
- Cordes J. M., Wasserman I., 2016, *MNRAS*, **457**, 232
- Cordes J. M., Wasserman I., Hessels J. W. T., Lazio T. J. W., Chatterjee S., Wharton R. S., 2017, *ApJ*, **842**, 35
- Cruces M., et al., 2020, *MNRAS*,
- Dai S., et al., 2020, arXiv e-prints, p. arXiv:2011.03960
- Desvignes G., et al., 2018, *ApJ*, **852**, L12
- Eftekhari T., Berger E., 2017, *ApJ*, **849**, 162
- Eftekhari T., Berger E., Williams P. K. G., Blanchard P. K., 2018, *ApJ*, **860**, 73
- Farah W., et al., 2018, *MNRAS*, **478**, 1209
- Fiedler R. L., Dennison B., Johnston K. J., Hewish A., 1987, *Nature*, **326**, 675
- Fonseca E., et al., 2020, *ApJ*, **891**, L6
- Gajjar V., et al., 2018, *ApJ*, **863**, 2
- Gourdji K., Michilli D., Spitler L. G., Hessels J. W. T., Seymour A., Cordes J. M., Chatterjee S., 2019, *ApJ*, **877**, L19
- Hankins T. H., Kern J. S., Weatherall J. C., Eilek J. A., 2003, *Nature*, **422**, 141
- Hardy L. K., et al., 2017, *MNRAS*, **472**, 2800
- Heintz K. E., et al., 2020, *ApJ*, **903**, 152
- Hessels J. W. T., et al., 2019, *ApJ*, **876**, L23
- Hewish A., Bell S. J., Pilkington J. D. H., Scott P. F., Collins R. A., 1968, *Nature*, **217**, 709
- Inoue S., 2004, *MNRAS*, **348**, 999
- Ioka K., 2003, *ApJ*, **598**, L79
- Ioka K., Zhang B., 2020, *ApJ*, **893**, L26
- James C. W., et al., 2020, *MNRAS*, **495**, 2416
- Joseph A., et al., 2019, *ApJ*, **882**, L18
- Kaspi V. M., Beloborodov A. M., 2017, *ARA&A*, **55**, 261
- Katz J. I., 2014, *Phys. Rev. D*, **89**, 103009
- Keane E. F., et al., 2018, *MNRAS*, **473**, 116
- Kirsten F., Snelders M. P., Jenkins M., Nimmo K., van den Eijnden J., Hessels J. W. T., Gawroński M. P., Yang J., 2020, *Nature Astronomy*,
- Kouveliotou C., Meegan C. A., Fishman G. J., Bhat N. P., Briggs M. S., Koshut T. M., Paciesas W. S., Pendleton G. N., 1993, *ApJ*, **413**, L101
- Kumar P., Lu W., Bhattacharya M., 2017, *MNRAS*, **468**, 2726
- Kumar P., et al., 2021, *MNRAS*, **500**, 2525
- Law C. J., et al., 2020, *ApJ*, **899**, 161
- Levin Y., Beloborodov A. M., Bransgrove A., 2020, *ApJ*, **895**, L30
- Lin L., et al., 2020, *Nature*, **587**, 63
- Linscott I. R., Erkes J. W., 1980, *ApJ*, **236**, L109
- Loeb A., Shvartzvald Y., Maoz D., 2014, *MNRAS*, **439**, L46
- Lorimer D. R., Bailes M., McLaughlin M. A., Narkevic D. J., Crawford F., 2007, *Science*, **318**, 777
- Lu W., Kumar P., Zhang B., 2020, *MNRAS*, **498**, 1397
- Luo R., et al., 2020, *Nature*, **586**, 693
- Lyubarsky Y., 2014, *MNRAS*, **442**, L9
- Lyutikov M., Barkov M. V., Giannios D., 2020, *ApJ*, **893**, L39
- Macquart J. P., et al., 2020, *Nature*, **581**, 391
- Manchester R. N., Hobbs G. B., Teoh A., Hobbs M., 2005, *AJ*, **129**, 1993
- Maoz D., et al., 2015, *MNRAS*, **454**, 2183
- Marcote B., et al., 2017, *ApJ*, **834**, L8
- Marcote B., et al., 2020, *Nature*, **577**, 190
- Margalit B., Metzger B. D., 2018, *ApJ*, **868**, L4
- Margalit B., Metzger B. D., Sironi L., 2020a, *MNRAS*, **494**, 4627
- Margalit B., Beniamini P., Sridhar N., Metzger B. D., 2020b, *ApJ*, **899**, L27
- Masui K., et al., 2015, *Nature*, **528**, 523
- McLaughlin M. A., et al., 2006, *Nature*, **439**, 817
- McQuinn M., 2014, *ApJ*, **780**, L33
- Michilli D., et al., 2018, *Nature*, **553**, 182
- Muñoz J. B., Kovetz E. D., Dai L., Kamionkowski M., 2016, *Phys. Rev. Lett.*, **117**, 091301
- Ocker S. K., Cordes J. M., Chatterjee S., 2020, *ApJ*, **897**, 124
- Petroff E., et al., 2015a, *MNRAS*, **447**, 246
- Petroff E., et al., 2015b, *MNRAS*, **454**, 457
- Petroff E., et al., 2017, *MNRAS*, **469**, 4465
- Petroff E., Hessels J. W. T., Lorimer D. R., 2019, *A&ARv*, **27**, 4
- Platts E., Weltman A., Walters A., Tendulkar S. P., Gordin J. E. B., Kandhai S., 2019, *Phys. Rep.*, **821**, 1
- Price D. C., et al., 2019, *MNRAS*, **486**, 3636
- Prochaska J. X., Zheng Y., 2019, *MNRAS*, **485**, 648
- Prochaska J. X., et al., 2019, *Science*, **366**, 231

- Rajwade K. M., et al., 2020, *MNRAS*, 495, 3551
- Ravi V., 2019a, *Nature Astronomy*, 3, 928
- Ravi V., 2019b, *MNRAS*, 482, 1966
- Ravi V., et al., 2016, *Science*, 354, 1249
- Ravi V., et al., 2019a, *BAAS*, 51, 420
- Ravi V., et al., 2019b, *Nature*, 572, 352
- Scholz P., et al., 2016, *ApJ*, 833, 177
- Shannon R. M., et al., 2018, *Nature*, 562, 386
- Sob'yanin D. N., 2020, *MNRAS*, 497, 1001
- Spitler L. G., et al., 2014, *ApJ*, 790, 101
- Spitler L. G., et al., 2016, *Nature*, 531, 202
- Tavani M., et al., 2020, arXiv e-prints, p. arXiv:2005.12164
- Taylor J. H., Cordes J. M., 1993, *ApJ*, 411, 674
- Tendulkar S. P., et al., 2017, *ApJ*, 834, L7
- Tendulkar S. P., et al., 2020, arXiv e-prints, p. arXiv:2011.03257
- Thornton D., et al., 2013, *Science*, 341, 53
- Vachaspati T., 2008, *Phys. Rev. Lett.*, 101, 141301
- Vieyro F. L., Romero G. E., Bosch-Ramon V., Marcote B., del Valle M. V., 2017, *A&A*, 602, A64
- Walters A., Weltman A., Gaensler B. M., Ma Y.-Z., Witzemann A., 2018, *ApJ*, 856, 65
- Weltman A., Walters A., 2020, *Nature*, 587, 43
- Yao J. M., Manchester R. N., Wang N., 2017, *ApJ*, 835, 29
- Zackay B., Ofek E. O., 2017, *ApJ*, 835, 11
- Zanazzi J. J., Lai D., 2020, *ApJ*, 892, L15
- Zhang B., 2017, *ApJ*, 836, L32
- Zhang B., 2020, *Nature*, 587, 45
- Zhang Y. G., Gajjar V., Foster G., Siemion A., Cordes J., Law C., Wang Y., 2018, *ApJ*, 866, 149

This paper has been typeset from a $\text{\TeX}/\text{\LaTeX}$ file prepared by the author.